HHS Public Access

Author manuscript

Dev Dyn. Author manuscript; available in PMC 2021 October 04.

Published in final edited form as:

Dev Dyn. 2021 October ; 250(10): 1450–1462. doi:10.1002/dvdy.326.

Eya2 expression during mouse embryonic development revealed by *Eya2*^{lacZ} knockin reporter and homozygous mice show mild hearing loss

Ting Zhang[1], **Jinshu Xu**[1], **Pin-Xian Xu**[1,2]

[1]Department of Genetics and Genomic Sciences, Icahn School of Medicine at Mount Sinai, New York, New York

[2]Department of Cell, Developmental and Regenerative Biology, Icahn School of Medicine at Mount Sinai, New York, New York

Abstract

Background: *Eya2* expression during mouse development has been studied by in situ hybridization and it has been shown to be involved skeletal muscle development and limb formation. Here, we generated *Eya2* knockout (*Eya2*$^{-}$) and a *lacZ* knockin reporter (*Eya2*^{lacZ}) mice and performed a detailed expression analysis for *Eya2*^{lacZ} at different developmental stages to trace *Eya2*^{lacZ}-positive cells in *Eya2*-null mice. We describe that *Eya2* is not only expressed in cranial sensory and dorsal root ganglia, retina and olfactory epithelium, and somites as previously reported, but also *Eya2* is specifically detected in other organs during mouse development.

Results: We found that *Eya2* is expressed in ocular and trochlear motor neurons. In the inner ear, *Eya2*^{lacZ} is specifically expressed in differentiating hair cells in both vestibular and cochlear sensory epithelia of the inner ear and *Eya2*$^{-/-}$ or *Eya2*$^{lacZ/lacZ}$ mice displayed mild hearing loss. Furthermore, we detected *Eya2* expression during both salivary gland and thymus development and *Eya2*-null mice had a smaller thymus.

Conclusions: As *Eya2* is coexpressed with other members of the Eya family genes, these results together highlight that *Eya2* as a potential regulator may act synergistically with other Eya genes to regulate the differentiation of the inner ear sensory hair cells and the formation of the salivary gland and thymus.

Keywords

cranial placodes; cranial sensory ganglia; *Eya2* ; hearing loss; inner ear hair cells; neural crest cells; ocular/trochlear motor neurons; salivary gland; sensory organs; thymus

Correspondence: Pin-Xian Xu, Ph.D., 1425 Madison Ave, Icahn Building, Rm 14-20D, New York, NY 10029. pinxian.xu@mssm.edu.

AUTHOR CONTRIBUTIONS

Ting Zhang: Data curation; formal analysis; investigation; validation; writing-original draft; writing-review & editing. **Pin-Xian Xu:** Conceptualization; formal analysis; funding acquisition; investigation; methodology; project administration; supervision; visualization; writing-original draft; writing-review & editing. **jinshu Xu:** Data curation; formal analysis; methodology; validation; writing-review & editing.

1 | INTRODUCTION

Eya2 is a member of the Eyes absent (Eya) family proteins, which are defined by the presence of a highly conserved 271 amino acid carboxyl terminal Eya domain (ED).[1] The conserved ED of Eya not only participates in protein-protein interactions but also possesses a catalytic motif belonging to the phosphatase subgroup of the haloacid dehalogenase (HAD) superfamily of enzymes,[2–4] while the divergent N-terminus of Eya possesses a transcriptional activation function.[5] In *Drosophila*, Eya has a critical role in eye formation and *eya* mutation causes progenitor cells in the eye imaginal disc to undergo programmed cell death.[6] Eya functions in a regulatory network important to eye formation, including eyeless (Ey), sine oculis (So), and dachshund (Dac), all of which have at least some ability to direct ectopic eye formation and are part of a complex feedback loop that regulates their own expression.[7–12]

Four different Eya genes (*Eya1–4*) have been isolated in mouse and human.[1,13–16] A number of studies have shown that overexpression of all four human *EYA1–4* genes has been associated with various cancers, including colorectal cancer, epithelial ovarian cancer, lung cancer, prostate cancer and breast cancer,[17–21] while overexpression studies in transgenic mice have implicated a role for *Eya2* in cardiac hypertrophy.[22,23] Mutations in the human *EYA1* cause branchio-oto-renal (BOR) or branchio-otic (BO) syndrome[16] and sporadic cases of congenital cataracts and ocular anterior segment anomalies.[24] On the other hand, the majority of *EYA4* mutations are associated with autosomal dominant non-syndromic sensorineural hearing loss (DFNA10) and mild cardiac phenotype.[25–27] In contrast, *EYA2* and *EYA3* have not yet been linked to any human syndromes. Loss of function studies in mice have revealed essential function for *Eya1* in multiple organ systems including the cranial sensory neurogenesis, inner ear, parathyroid, thymus and kidney[28–30] and *Eya4* in otitis media.[31] In contrast, loss of *Eya3* in mice displayed a broad spectrum of minor physiological changes, including decreased bone mineral content and shorter body length.[32] We have generated *Eya2* knockout mice and *Eya2*-null mice are viable and fertile without obvious external phenotype. This could be due to a functional redundancy with other members of the Eya family genes, which is supported by the observation that *Eya2* has a synergistic role with *Eya1* during somatic myogenic precursor cell differentiation.[33] Consistent with this view, overlapping expression of both *Eya2* and *Eya1* was observed in multiple tissues in a mouse embryo, including cranial sensory structures, myogenic precursors and connective precursor cells in the limb.[1,5] Interestingly, a recent study reported that deletion of *eya2* in axolotl through CRISPR/Cas9 impairs cell cycle progression and results in elevated DNA damage in the limb.[34] However, a systematic analysis of the functional role of *Eya2* during mouse development and its potential redundancy with other Eya family members is still lacking.

Our previous in situ hybridization detected that at E9.5–10.5, *Eya2* is predominantly expressed in sensory structures in the head, including the cranial sensory ganglia and olfactory placode. At E12.5–E14.5, *Eya2* expression is maintained in the olfactory epithelium and becomes detectable in the retina, sclera and optic nerve sheath.[1] However, it remains unclear whether *Eya2*-expressing cranial sensory ganglia at E9.5–10.5 in the head is neural crest cell (NCC)- and/or ectodermal placode-derived cells. Furthermore,

it is not known whether *Eya2* could be a potential regulator of other cranial sensory or developmental processes during mouse organogenesis.

To address this, in addition to the *Eya2* knockout (KO) mice, we generated a *lacZ* knockin (KI) reporter mice and performed β-Gal staining for the $Eya2^{lacZ}$ on whole embryos or sections at different stages of development and traced the β-Gal-positive cells in $Eya2^{lacZ/lacZ}$ homozygotes. Here, we show that *Eya2* is exclusively expressed in NCC-derived components of cranial sensory ganglia Vth, VIIth, VIIIth, IXth and IXth, and in other sensory and developmental systems that have not been reported so far: ocular/trochlear motor neurons, inner ear, salivary gland and thymus. We describe that during inner ear development, β-Gal activity is specifically accumulated in differentiating sensory hair cells of all sensory patches and that both $Eya2^{lacZ/lacZ}$ or $Eya2^{-/-}$ mice displayed mild hearing loss. During salivary gland development, β-Gal is expressed in the initial epithelial bud as thickening of the primitive oral epithelium and later during branching morphogenesis, β-Gal is stronger in the lumenized main duct and weaker in the end buds. Moreover, we show that during thymus development, β-Gal is expressed in the parathyroid/thymus primordium of the third pharyngeal pouch endoderm, but later on its expression becomes restricted to the thymus lobes. In the *Eya2* homozygotes, the thymic lobes appear smaller in size compared to the heterozygous controls. Altogether, these results complete a study describing the generation of *Eya2* KO and $Eya2^{lacZ}$ KI mice and the expression of *Eya2* revealed by the $Eya2^{lacZ}$ reporter in both vestibular and cochlear hair cells as well as developing salivary gland and thymus. This work reveals a potential role for *Eya2* in these structures. The $Eya2^{lacZ}$ mice generated here can be used as a tool for further systematically investigating the differentiation and maintenance of *Eya2*-expressing cells in different organ systems.

2 | RESULTS AND DISCUSSION

2.1 | Generation of *Eya2* knockout and $Eya2^{lacZ}$ knockin alleles

To inactivate the *Eya2* gene, we generated a null allele by replacing exons 11 encoding 55 residues of the conserved 271-amino acid ED domain (Figure 1A, see Experimental Procedures), which mediates protein-protein interactions and possesses intrinsic phosphatase activity. $Eya2^{-/-}$ mice were fertile with normal appearance, suggesting that there may be functional redundancy with other members of the Eya family genes. Consistent with this view, analysis of muscle development found that both *Eya1* and *Eya2* function synergistically and are necessary for hypaxial somitic myogenesis in the mouse embryo, as *Pax3* expression is lost in the ventrolateral (hypaxial) dermomyotomes of the somite in $Eya1^{-/-}$; $Eya2^{-/-}$ mice.[33] In order to follow the fate of the cells after *Eya2* depletion, we generated a $Eya2^{lacZ}$ knockin allele by homologous recombination in ES cells to replace exon 2, which contains the endogenous start codon of Eya2, with a promoterless ATG-lacZ-poly(A) cassette and the *PGK-neo* gene (Figure 1B). Germline transmission of the targeted allele was confirmed by southern blot with a 5′ flanking probe and PCR using a common forward primer in the intron 1 and a reverse primer within the exon2 or within the lacZ gene for detecting *Eya2* wild-type or *lacZ* knockin allele (Figure 1C,D). Similar to $Eya2^{-/-}$ mice, all $Eya2^{lacZlacZ}$ mice are fertile without obvious external phenotype.

As the *lacZ* reporter gene is driven by the endogenous *Eya2* promoter, we next performed β-Gal staining for the expression of $Eya2^{lacZ}$ allele and found β-Gal activity in the nose, eye, ocular (III) and trochlear (IV) motor neurons, Rathke's pouch, cranial sensory ganglia—the trigeminal (V), facioacoustic (VII–VIII), glossopharyngeal (IX) and vagus (X) ganglia—and the dorsal root ganglion (Figure 1E,E′). As expected, $Eya2^{lacZ/lacZ}$ homozygotes displayed similar pattern of β-Gal expression with stronger β-Gal activity compared to heterozygotes (Figure 1F, F′). This pattern recaptured the pattern of endogenous *Eya2* expression detected by in situ hybridization.[1] Thus, these mice provide a valuable model for assessing *Eya2* expression and tracing the cells after *Eya2* depletion.

The sensory ganglia in the vertebrate head are composed of neural crest cell (NCC)-derived neurons and glia and ectodermal placode-derived neurons. The trigeminal and epibranchial (geniculate, petrosal, and nodose) placodes produce neuronal precursor cells that directly delaminate to contribute sensory neurons to the distal part of the Vth (trigeminal) and of the VIIth (geniculate), IXth (petrosal) and Xth (nodose) cranial nerves respectively, whereas the NCCs produce the proximal components and associated glia of these cranial nerves.[35,36] The VIIIth (vestibuloacoustic) ganglion is composed of the otic placode-derived neurons and NCC-derived glia and some neurons.[37] We observed *Eya2* expression in a subset of cranial placodes—the neurogenic olfactory placode[1,38] and the non-neurogenic placode-derived Rathke's pouch (Figure 1E), but not in the non-neurogenic lens[1] and neurogenic otic placode-derived otocyst (Figure 1E), which differentiates into all inner ear structures. Although *Eya2* is strongly expressed in all cranial ganglia, it remains unclear whether *Eya2*-expressing cells in the Vth, VIIth, IXth and Xth are derived from NCCs, placodes or both. As the NCCs migrate from the neuroectoderm and $Eya2^{lacZ}$ is expressed in the dorsal tip of the neural tube and migratory NCCs (asterisk in Figure 1E), we thus hypothesized that *Eya2* expression may be restricted to or predominantly in NCC-derived parts of the Vth, VIIth, VIIIth, IXth and Xth ganglia. To test this, we performed X-gal staining at E9.5 when the thickened placodes, which are transient structures, are readily detectable. At E9.5, $\beta\text{-Gal}^+$ cells were detected in Vth, VIIth and VIIIth ganglia, while fewer $\beta\text{-Gal}^+$ cells were observed in the XIth and Xth ganglionic regions (Figure 1G). On sections, β-Gal activity was observed in the trigeminal placodal ectoderm (Figure 1G′) and Vth ganglion (Figure 1G″), whereas $\beta\text{-Gal}^+$ cells were not observed in epibranchial placode (arrow, Figure 1G‴) or otocyst (Figure 1G‴). In addition to NCC-derived components of the VIIth and VIIIth ganglia (Figure 1F′), we observed $\beta\text{-Gal}^+$ cells in the mesenchyme surrounding the otocyst or migratory cells in the VIIth ganglionic region. Thus, in addition to the NCC-derived parts of cranial sensory ganglia, $Eya2^{lacZ}$ may be expressed in some differentiating neuronal progenitors that have delaminated from the otocyst or epibranchial placodal ectoderm. The selective expression of *Eya2* in the ocular and trochlear motor neurons suggests that Eya2 may have a role in these motor neuron development. Previous studies have shown unique expression of several factors, including Phox2b, Wnt1 and Lmx1b,[39] in the ocular and trochlear motor neurons. Further characterization of the Eya family gene expression and their functional redundancy in these motor neurons will reveal the potential relationship of Eya genes with other regulators during ocular and trochlear motor nerve development.

2.2 | Expression of *Eya2* in olfactory epithelium, eye, dorsal root ganglion and somite

Consistent with our previous observation obtained by in situ hybridization,[1,38] strong β-Gal activity was observed in the olfactory placode and invaginating olfactory epithelium at E9.5–10.5 (Figure 1E,F,G,G′). At E12.5, *Eya2*^{lacZ} was strongly expressed in the olfactory system (Figure 2A). The olfactory placode is a neurogenic placode and it differentiates into neuronal and non-neuronal cells in the olfactory system. The mammalian olfactory epithelium (OE) is composed of sensory neurons, which are generated in the basal region and extend apically to the nasal cavity, and an apical layer of glial-like sustentacular cells (Figure 2B).[40,41] X-gal staining on OE sections from E14.5 revealed that β-Gal activity is restricted to the neuronal progenitors in the basal layer but not in the sustentacular cells in the apical layer of the OE (Figure 2B). β-Gal activity was also detected in the vomeronasal organ (VNO) (Figure 2C). There was no obvious difference in the expression levels of *Eya2*^{lacZ} in the OE between *Eya2*$^{lacZ/+}$ and *Eya2*$^{lacZ/lacZ}$. As in mammals, initial detection of olfactory stimuli is mediated by sensory neurons in the OE and VNO, the expression of *Eya2* in the olfactory sensory neurons suggests that Eya2 may be involved in olfactory sensory neurogenesis.

The lens is non-neurogenic and differentiates into both lens fiber and lens epithelial cells.[42,43] *Eya2* expression was not detected in the lens placode at E9.5–10.5.[1] Consistent with this, *Eya2*^{lacZ} expression was also not observed in lens development at any stages, while whole mount revealed *Eya2*^{lacZ} expression in the mesenchyme around the eye (Figure 1E). In the retina, X-gal staining of *Eya2*^{lacZ} at E12.5 showed β-Gal activity in *Eya2*$^{lacZ/+}$ and *Eya2*$^{lacZ/lacZ}$ (Figure 2D). By E14.5, β-Gal activity is restricted to the inner nuclear layer of the retina with similar intensity between *Eya2*$^{lacZ/+}$ and *Eya2*$^{lacZ/lacZ}$ (Figure 2E). β-Gal activity was also observed in the sclera, extraocular muscles, and nerve fibers within the optic stalk, which will develop into optic (II) nerve (Figure 2D,E). This is consistent with our previous observation detected by in situ hybridization.[1]

In addition, β-Gal activity was observed in limb tendons (Figure 2A), dorsal root ganglion and somite with stronger intensity in the homozygotes compared to the heterozygotes (Figure 2F). Altogether these data support that *Eya2* may have a role in olfactory and retinal neuronal differentiation, dorsal root ganglion, limb and somite.

2.3 | *Eya2* is expressed in differentiating sensory hair cells of all inner ear sensory organs

While *Eya2* expression was not observed in the otic ectoderm at earlier stages its expression during inner ear development at later stages has not been examined. To analyze whether *Eya2* could be a potential regulator in the inner ear or other developmental processes, we performed detailed X-gal staining to detect *Eya2*^{lacZ} expression during mouse embryogenesis. During inner ear development, the sensory progenitors are specified within the ventral region of the otocyst at E10.5 and proliferate to expand. After reaching a defined number, they undergo differentiation in the vestibule around E12.5 and in cochlea around E14.5 to form sensory hair cells or underlying supporting cells within each sensory epithelium in the inner ear. X-gal staining of *Eya2*^{lacZ} at E9.5–12.5 failed to detect β-Gal activity in the otic epithelium of either heterozygotes or homozygotes (Figure 3A). In

contrast, *Eya2*^{lacZ} expression persists in the dorsal neural tube and the sensory ganglia of Vth, VIIth, VIIIth, IXth, Xth nerves and cranial and spinal part of the accessory (XI) nerve with weaker β-Gal activity in the heterozygotes and stronger activity in homozygotes (Figure 3A). By E14.5–15.5, β-Gal activity was readily detected in the differentiating sensory hair cells of all five vestibular sensory organs, the macula of utricle and saccule and the crista ampullaris of each of the semicircular canals in both *Eya2*$^{lacZ/+}$ and *Eya2*$^{lacZ/lacZ}$ (Figure 3B,C). The differentiation of the sensory organ for hearing (the organ of Corti) in the cochlea occurs E14.5 in mid-basal region toward base and apex and medial-to-lateral (inner-to-outer hair cell) directions. β-Gal activity became detectable in the organ of Corti of the basal cochlea (bracket, Figure 3B,D). As differentiation proceeds, β-Gal activity became progressively detectable toward apex and reached apex by E18.5 in both inner and outer hair cells (Figure 3D).

The vestibuloacoustic VIIIth ganglion differentiates into vestibular and spiral ganglion. We observed β-Gal activity in the vestibular ganglion but not in the spiral ganglion neurons (Figure 3B,D). Some β-Gal activity was observed in cells surrounding the spiral ganglion neurons in the cochlea (Figure 3D). Thus, it is possible that *Eya2* is specifically turned on in a subset of differentiating VIIIth ganglion neuronal progenitors that will differentiate into vestibular ganglion neurons. Our results also indicate that *Eya2* expression is specifically turned on in the differentiating hair cells of all six sensory epithelia in the inner ear.

2.4 | *Eya2*$^{lacZ/lacZ}$ mice exhibit hearing loss

Eya2$^{lacZ/lacZ}$ or *Eya2*$^{-/-}$ mice do not exhibit vestibular dysfunction such as headtossing or circling behavior, but some homozygotes showed a weaker response to Preyer reflex test (Figure 4A). We therefore used measurements of auditory brainstem response (ABR) thresholds to assess hearing deficiency of *Eya2*$^{lacZ/lacZ}$ mice and the control heterozygous littermates at 8 weeks of age. Compared to the baseline, ABR thresholds were significantly elevated in frequency stimuli ranging from 5.6 to 45.2 kHz in *Eya2*$^{lacZ/lacZ}$ mice ($n = 7$) compared with control littermates ($n = 5$) (Figure 4B), while 3 mice (one male and two females) had no ABR response. There were no statistically significant differences between the right and left ears or male and female animals.

We have previously reported that no inner ear structure forms in *Eya1*$^{-/-}$ mice[28] and no inner ear hair cell formation in *Eya1* conditional mutant mice when Eya1 was deleted at later stages.[44] Thus, while Eya1 has an early role in inner ear development, Eya2 may have a redundant role with Eya1 specifically in differentiating hair cells.

2.5 | *Eya2* is expressed in salivary gland development

Interestingly, we also detected β-Gal activity in the salivary gland (Figure 5), which was also not reported previously. The salivary gland contains three major types—submandibular (SMG) secreting seromucous saliva, sublingual (SLG) secreting mucous saliva, and parotid (PG) secreting serous saliva, all of which arose as epithelial buds in the oral cavity. Among them, the SMG is the most commonly studied and the SMG bud forms around E12.5 in mice.[45] At this stage, very faint β-Gal activity was only observed in the PG bud region in *Eya2*$^{lacZ/+}$ (Figure 5A). In *Eya2*$^{lacZ/lacZ}$, β-Gal activity appeared stronger in the PG bud

region, and weaker in the SMG bud (Figure 5A). The bud undergoes branching to produce a cluster of branches and buds, which continue branching to produce a multi-lobed gland by E14.5. The main duct begins to lumenize, while the end buds undergo reorganization and begin to form acini—the main secretory units of the salivary gland. At E14.5, β-Gal activity was observed in all three types of the salivary glands, with stronger intensity in the initial duct (Figure 5B–D). These data suggest that *Eya2* may have a role in salivary gland development or function.

Detailed analyses of expression of other members of the Eya gene family and loss of function studies in compound mutant during salivary gland development and branching morphogenesis will provide molecular basis of salivary gland branching morphogenesis. The $Eya2^{lacZ}$ mice may serve as a tool for a systematic level understanding of salivary gland development.

2.6 | *Eya2* is expressed during thymus development and $Eya2^{lacZ/lacZ}$ mice exhibit smaller thymus

In addition to the salivary gland, we also observed *Eya2* expression in thymus development for the first time (Figure 6). The thymus is the primary organ responsible for generating functional T cells in vertebrates and it develops from the third pharyngeal pouch primordium. The third pouch evaginates at E10.5 to form the primordia of thymus/parathyroid at around E12.5 and β-Gal activity was detectable in the primordium at these stages in both $Eya2^{lacZ/+}$ and $Eya2^{lacZ/lacZ}$ embryos (Figure 6A and data not shown). At E13.5 and E14.5, the parathyroid have separated from thymus lobes, which continue to descend toward midline, *Eya2* showed thymus-restricted expression at these stages (Figure 6B). In $Eya2^{lacZ/lacZ}$ embryos, the thymic primordia formed, detached from the pharynx and migrated to their normal position above the heart (Figure 6B). However, from the E15.5 sections we noted that the two thymus lobes in $Eya2^{lacZ/lacZ}$ embryos were smaller compared to $Eya2^{lacZ/+}$ littermates (Figure 6C). To confirm the size reduction, we dissected out the whole thymus lobes at P0 and found that $Eya2^{lacZ/lacZ}$ thymus was apparently smaller compared to heterozygous thymus (Figure 6D), suggesting that Eya2 may have a role during thymus differentiation.

We have previously reported that *Eya1* is expressed in the pharyngeal endoderm from as early as E9.5 and in the primordium of and later in both parathyroid and thymus.[30] *Eya1* is required early for both parathyroid and thymus development as the primordium of parathyroid/thymus failed to form in $Eya1^{-/-}$ mice.[30] Eya2 may have a synergistic role with Eya1 to specifically regulate thymus development and differentiation. Analyzing whether different lineages of thymic cells develop normally in the absence of *Eya2* or in *Eya1;Eya2* compound mutant mice will shed light on the functional roles of *Eya2* and *Eya1* in thymus differentiation and function.

3 | CONCLUSIONS

In this study, we report the generation of targeted knockout and lacZ reporter knockin alleles for the mouse *Eya2* gene and performed a detailed analysis of *Eya2* expression and its potential role during mouse development. $Eya2^{lacZ}$ expression recaptured *Eya2* mRNA

expression in the cranial sensory ganglia, olfactory epithelium, dorsal root ganglion, limb tendons, and somatic myogenic precursors previously detected by in situ hybridization. We report here our novel finding that *Eya2*-expressing cells in the sensory ganglia (Vth, VIIth, VIIIth, IXth, and Xth) are predominately derived from NCCs and that only small portion of them are neuronal progenitors delaminated from a subset of ectoderm placodes. Furthermore, we found that *Eya2* is expressed in the ocular and trochlear motor neurons, differentiating hair cells of both vestibular and cochlear sensory organs, and developing salivary gland and thymus. While $Eya2^{lacZ}$ expression in the homozygous organs depicted no difference with the heterozygous littermates, we found mild phenotypes in thymus and hearing due to *Eya2* depletion. As the Eya family proteins are widely expressed in embryogenesis, there is likely a redundancy with other *Eya* genes, which can substitute for the loss of *Eya2*. The $Eya2^{lacZ}$ allele generated here could assist further investigation of the potential functions of *Eya2* and its redundancy with other Eya genes by sorting the $Eya2^{lacZ}$-positive cells for transcriptome profiling to identify differentially expressed genes and transcriptomic pathways regulated by Eya2 alone or combination with other Eya genes.

4 | EXPERIMENTAL PROCEDURES

4.1 | Gene targeting and animals

We isolated *Eya2* genomic clones encoding the Eya domain from a 129/SvJ BAC genomic library and generated the targeting vector by ligation of a 3′ arm (3.8-kb XbaI fragment) and a 5′ arm (3.1-kb KpnI-HindII fragment) flanking a neo cassette into the vector pPNT. In the resulting plasmid (pPNT-Eya2), neo and tk are in opposite orientation with regard to Eya2. Correct targeting resulted in deletion of a 1.3-kb HindIII-XbaI fragment from 292 bp upstream to 850 bp downstream of exon 11 in the Eya domain region and replacement with pgk-neo. The targeting construct was linearized with NotI, electroporated into R1 ES cells and selected with G418 and FIAU. We identified two independent homologous recombinant ES lines by Southern blot using a 5′ external probe (0.5-kb EcoRI-Kpn1 fragment) and obtained four chimaeras by blastocyst injection that yielded germline transmission. Heterozygous or homozygous progeny were genotyped by PCR using a common forward primer (5′-TTAGCTTCAGGTAGCTGCTC-3′) and either of two allele-specific reverse primers (wild type, 5′-ACACATCTTGTCCCAGAACG-3′; Eya2neo, 5′-CAAGCAAAACCAAATTAAGGG-3′) in same or separate reactions to generate 230- and 250-bp amplicons, respectively.

For $Eya2^{lacZ}$ knockin, the same targeting vector was used and ES transfection, generation of chimeric mice and germline transmission were similarly performed. Heterozygous or homozygous progeny were genotyped by PCR using forward and reverse primers: WT forward primer: 5′-CTGAGTGACAGGGAAGGTAGG 3′; WT reverse primer: 5′-CTTCCTTGACTTCAACCCAAC-3′; mutant forward primer: 5′-TTGGGAATAGGTAATCAGCTT-3′; mutant reverse primer: 5′-TCTTCGCTATTACGCCAGCTG-3′. $Eya2^{+/-}$, $Eya2^{-/-}$ or $Eya2^{lacZ}$ mice were maintained on a 129/Sv and C57BL/6J mixed background. All animal protocols were approved by Animal Care and Use Committee of the Icahn School of Medicine at Mount Sinai (protocols #06–0807 and #06–0822).

4.2 | β-Gal staining

Mice were anesthetized with isoflurane and transcardially perfused with phosphate-buffered saline (PBS), followed by 4% paraformaldehyde (PFA). Embryos or tissue organs were fixed with 4% PFA for 0.5 hour, cryoprotected in 30% sucrose overnight, embedded in OCT compound (Tissue-Tek; Sakura Finetek USA), and sectioned on a cryotome at 10 μm thickness. Sections were air dried, rinsed in PBS, and stained in 0.8 mg/mL X-gal in 35 mM $K_3Fe(CN)_6$, 35 mM$K_4Fe(CN)_6$, and 2 mM $MgCl_2$ in PBS at room temperature until the blue staining appears. Sections were dehydrated through serial graded ethanol, cleared in xylenes, and cover slipped with permount. For whole mount staining, the embryos were fixed with 4% PFA for 0.5 hour, rinsed in PBS, and stained with the chemicals listed above.

4.3 | Preyer reflex test using a click box

The click-box hearing test elicits a Preyer reflex in hearing mice and provides a convenient, fast, low-cost phenotypic screen. The click box produces an 18.9-kHz burst of 106-dB sound pressure levels (SPLs) at a distance of 10 cm (Institute of Hearing Research, Nottingham, UK).

4.4 | Auditory-evoked brainstem response (ABR) testing

Eya2^{lacZ}/lacZ and control littermates were tested for hearing thresholds via ABR. A computer-assisted evoked potential system (Tucker-Davis technologies) was used to obtain ABR thresholds for tone pips at frequencies of 5, 8, 11, 16, 22.6, 32, and 45.2 kHz (tone pip duration 5 ms; repetition rate 30/s) and averaged responses to 512 pips of alternating polarity as described before.[46]

ACKNOWLEDGMENTS

We thank past and present lab members for their assistance in the maintenance of *Eya2* KO and *Eya2*^{lacZ} KI mouse lines. This work is supported by NIH RO1DC014718 and DK064640 (PXX).

Funding information

National Institute of Diabetes and Digestive and Kidney Diseases, Grant/Award Number: DK064640; National Institute on Deafness and Other Communication Disorders, Grant/Award Number: RO1DC014718

REFERENCES

1. Xu PX, Woo I, Her H, Beier DR, Maas RL. Mouse Eya homologues of the drosophila eyes absent gene require Pax6 for expression in lens and nasal placode. Development. 1997;124(1):219–231. [PubMed: 9006082]
2. Li X, Oghi KA, Zhang J, et al. Eya protein phosphatase activity regulates Six1-Dach-Eya transcriptional effects in mammalian organogenesis. Nature. 2003;426(6964):247–254. 10.1038/nature02083. [PubMed: 14628042]
3. Rayapureddi JP, Kattamuri C, Steinmetz BD, et al. Eyes absent represents a class of protein tyrosine phosphatases. Nature. 2003;426(6964):295–298. 10.1038/nature02093. [PubMed: 14628052]
4. Tootle TL, Silver SJ, Davies EL, et al. The transcription factor eyes absent is a protein tyrosine phosphatase. Nature. 2003;426 (6964):299–302. 10.1038/nature02097. [PubMed: 14628053]
5. Xu PX, Cheng J, Epstein JA, Maas RL. Mouse Eya genes are expressed during limb tendon development and encode a transcriptional activation function. Proc Natl Acad Sci U S A. 1997; 94(22):11974–11979. [PubMed: 9342347]

6. Bonini NM, Leiserson WM, Benzer S. The eyes absent gene: genetic control of cell survival and differentiation in the developing drosophila eye. Cell. 1993;72(3):379–395. [PubMed: 8431945]
7. Bonini NM, Bui QT, Gray-Board GL, Warrick JM. The drosophila eyes absent gene directs ectopic eye formation in a pathway conserved between flies and vertebrates. Development. 1997;124(23):4819–4826. [PubMed: 9428418]
8. Chen R, Amoui M, Zhang Z, Mardon G. Dachshund and eyes absent proteins form a complex and function synergistically to induce ectopic eye development in drosophila. Cell. 1997;91(7): 893–903. [PubMed: 9428513]
9. Pignoni F, Hu B, Zavitz KH, Xiao J, Garrity PA, Zipursky SL. The eye-specification proteins so and Eya form a complex and regulate multiple steps in drosophila eye development. Cell. 1997;91(7):881–891. [PubMed: 9428512]
10. Shen W, Mardon G. Ectopic eye development in drosophila induced by directed dachshund expression. Development. 1997; 124(1):45–52. [PubMed: 9006066]
11. Halder G, Callaerts P, Flister S, Walldorf U, Kloter U, Gehring WJ. Eyeless initiates the expression of both sine oculis and eyes absent during drosophila compound eye development. Development. 1998;125(12):2181–2191. [PubMed: 9584118]
12. Heanue TA, Reshef R, Davis RJ, et al. Synergistic regulation of vertebrate muscle development by Dach2, Eya2, and Six1, homologs of genes required for drosophila eye formation. Genes Dev. 1999;13(24):3231–3243. [PubMed: 10617572]
13. Zimmerman JE, Bui QT, Steingrimsson E, et al. Cloning and characterization of two vertebrate homologs of the drosophila eyes absent gene. Genome Res. 1997;7(2):128–141. [PubMed: 9049631]
14. Duncan MK, Kos L, Jenkins NA, Gilbert DJ, Copeland NG, Tomarev SI. Eyes absent: a gene family found in several metazoan phyla. Mamm Genome. 1997;8(7):479–485. 10.1007/s003359900480. [PubMed: 9195991]
15. Borsani G, DeGrandi A, Ballabio A, et al. EYA4, a novel vertebrate gene related to drosophila eyes absent. Hum Mol Genet. 1999;8(1):11–23. [PubMed: 9887327]
16. Abdelhak S, Kalatzis V, Heilig R, et al. A human homologue of the drosophila eyes absent gene underlies branchio-Oto-renal (BOR) syndrome and identifies a novel gene family. Nat Genet. 1997;15(2):157–164. 10.1038/ng0297-157. [PubMed: 9020840]
17. Zou HZ, Harrington JJ, Shire AM, et al. Highly methylated genes in colorectal neoplasia: implications for screening. Cancer Epidemol Biomark. 2007;16(12):2686–2696. 10.1158/1055-9965.Epi-07-0518.
18. Zhang L, Yang N, Huang J, et al. Transcriptional coactivator drosophila eyes absent homologue 2 is up-regulated in epithelial ovarian cancer and promotes tumor growth. Cancer Res. 2005;65(3):925–932. [PubMed: 15705892]
19. Liu ZY, Zhao L, Song YS. Eya2 is overexpressed in human prostate cancer and regulates docetaxel sensitivity and mitochondrial membrane potential through AKT/Bcl-2 signaling. Biomed Res Int. 2019;2019:3808432. 10.1155/2019/3808432. [PubMed: 31317026]
20. Anantharajan J, Zhou HB, Zhang LD, et al. Structural and functional analyses of an allosteric EYA2 phosphatase inhibitor that has on-target effects in human lung cancer cells. Mol Cancer Ther. 2019;18(9):1484–1496. 10.1158/1535-7163.Mct-18-1239. [PubMed: 31285279]
21. Xu PX. The EYA-SO/SIX complex in development and disease. Pediatr Nephrol. 2013;28(6):843–854. 10.1007/s00467-012-2246-1. [PubMed: 22806561]
22. Lee SH, Yang DK, Choi BY, et al. The transcription factor Eya2 prevents pressure overload-induced adverse cardiac remodeling. J Mol Cell Cardiol. 2009;46(4):596–605. 10.1016/j.yjmcc.2008.12.021. [PubMed: 19272299]
23. Lee SH, Kim J, Ryu JY, et al. Transcription coactivator Eya2 is a critical regulator of physiological hypertrophy. J Mol Cell Cardiol. 2012;52(3):718–726. 10.1016/j.yjmcc.2011.12.002. [PubMed: 22197309]
24. Azuma N, Hirakiyama A, Inoue T, Asaka A, Yamada M. Mutations of a human homologue of the drosophila eyes absent gene (EYA1) detected in patients with congenital cataracts and ocular anterior segment anomalies. Hum Mol Genet. 2000;9(3): 363–366. [PubMed: 10655545]

25. Abe S, Takeda H, Nishio SY, Usami SI. Sensorineural hearing loss and mild cardiac phenotype caused by an EYA4 mutation. Hum Genome Variat. 2018;5:23;5:23.10.1038/s41439-018-0023-9.
26. Morin M, Borreguero L, Booth KT, et al. Insights into the pathophysiology of DFNA10 hearing loss associated with novel EYA4 variants. Sci Rep. 2020;10(1):6213. 10.1038/s41598-020-63256-5. [PubMed: 32277154]
27. Makishima T, Madeo AC, Brewer CC, et al. Nonsyndromic hearing loss DFNA10 and a novel mutation of EYA4: evidence for correlation of normal cardiac phenotype with truncating mutations of the Eya domain. Am J Med Genet A. 2007;143A(14):1592–1598. 10.1002/ajmg.a.31793. [PubMed: 17567890]
28. Xu PX, Adams J, Peters H, Brown MC, Heaney S, Maas R. Eya1-deficient mice lack ears and kidneys and show abnormal apoptosis of organ primordia. Nat Genet. 1999;23(1):113–117. 10.1038/12722. [PubMed: 10471511]
29. Zou D, Silvius D, Fritzsch B, Xu PX. Eya1 and Six1 are essential for early steps of sensory neurogenesis in mammalian cranial placodes. Development. 2004;131(22):5561–5572. 10.1242/dev.01437. [PubMed: 15496442]
30. Xu PX, Zheng W, Laclef C, et al. Eya1 is required for the morphogenesis of mammalian thymus, parathyroid and thyroid. Development. 2002;129(13):3033–3044. [PubMed: 12070080]
31. Depreux FF, Darrow K, Conner DA, et al. Eya4-deficient mice are a model for heritable otitis media. J Clin Invest. 2008;118(2):651–658. 10.1172/JCI32899. [PubMed: 18219393]
32. Soker T, Dalke C, Puk O, et al. Pleiotropic effects in Eya3 knockout mice. BMC Dev Biol. 2008;8:118. 10.1186/1471-213X-8-118. [PubMed: 19102749]
33. Grifone R, Demignon J, Giordani J, et al. Eya1 and Eya2 proteins are required for hypaxial somitic myogenesis in the mouse embryo. Dev Biol. 2007;302(2):602–616. 10.1016/j.ydbio.2006.08.059. [PubMed: 17098221]
34. Sousounis K, Bryant DM, Fernandez JM, et al. Eya2 promotes cell cycle progression by regulating DNA damage response during vertebrate limb regeneration. Elife. 2020;9:e51217. 10.7554/elife.51217. [PubMed: 32142407]
35. Ayer-Le Lievre CS, Le Douarin NM. The early development of cranial sensory ganglia and the potentialities of their component cells studied in quail-chick chimeras. Dev Biol. 1982;94(2):291–310. 10.1016/0012-1606(82)90349-9. [PubMed: 7152108]
36. D'Amico-Martel A, Noden DM. Contributions of placodal and neural crest cells to avian cranial peripheral ganglia. Am J Anat. 1983;166(4):445–468. 10.1002/aja.1001660406. [PubMed: 6858941]
37. Freyer L, Aggarwal V, Morrow BE. Dual embryonic origin of the mammalian otic vesicle forming the inner ear. Development. 2011;138(24):5403–5414. 10.1242/dev.069849. [PubMed: 22110056]
38. Chen B, Kim EH, Xu PX. Initiation of olfactory placode development and neurogenesis is blocked in mice lacking both Six1 and Six4. Dev Biol. 2009;326(1):75–85. 10.1016/j.ydbio.2008.10.039. [PubMed: 19027001]
39. Jahan I, Kersigo J, Elliott KL, Fritzsch B. Smoothened overexpression causes trochlear motoneurons to reroute and innervate ipsilateral eyes. Cell Tissue Res. 2021. 10.1007/s00441-020-03352-0.
40. Holbrook EH, Szumowski KEM, Schwob JE. An immune-chemical, ultrastructural, and developmental characterization of the horizontal basal cells of rat olfactory epithelium. J Comp Neurol. 1995;363(1):129–146. 10.1002/cne.903630111. [PubMed: 8682932]
41. Whitby-Logan GK, Weech M, Walters E. Zonal expression and activity of glutathione S-transferase enzymes in the mouse olfactory mucosa. Brain Res. 2004;995(2):151–157. 10.1016/j.brainres.2003.09.012. [PubMed: 14672804]
42. Cvekl A, Duncan MK. Genetic and epigenetic mechanisms of gene regulation during lens development. Prog Retin Eye Res. 2007;26(6):555–597. 10.1016/j.preteyeres.2007.07.002. [PubMed: 17905638]
43. Lang RA. Pathways regulating lens induction in the mouse. Int J Dev Biol. 2004;48(8–9):783–791. 10.1387/ijdb.041903rl. [PubMed: 15558471]

44. Ahmed M, Wong EY, Sun J, Xu J, Wang F, Xu PX. Eya1-Six1 interaction is sufficient to induce hair cell fate in the cochlea by activating Atoh1 expression in cooperation with Sox2. Dev Cell. 2012;22(2):377–390. 10.1016/j.devcel.2011.12.006. [PubMed: 22340499]

45. Tucker AS. Salivary gland development. Semin Cell Dev Biol. 2007;18(2):237–244. 10.1016/j.semcdb.2007.01.006. [PubMed: 17336109]

46. Zheng W, Huang L, Wei ZB, Silvius D, Tang B, Xu PX. The role of Six1 in mammalian auditory system development. Development. 2003;130(17):3989–4000. [PubMed: 12874121]

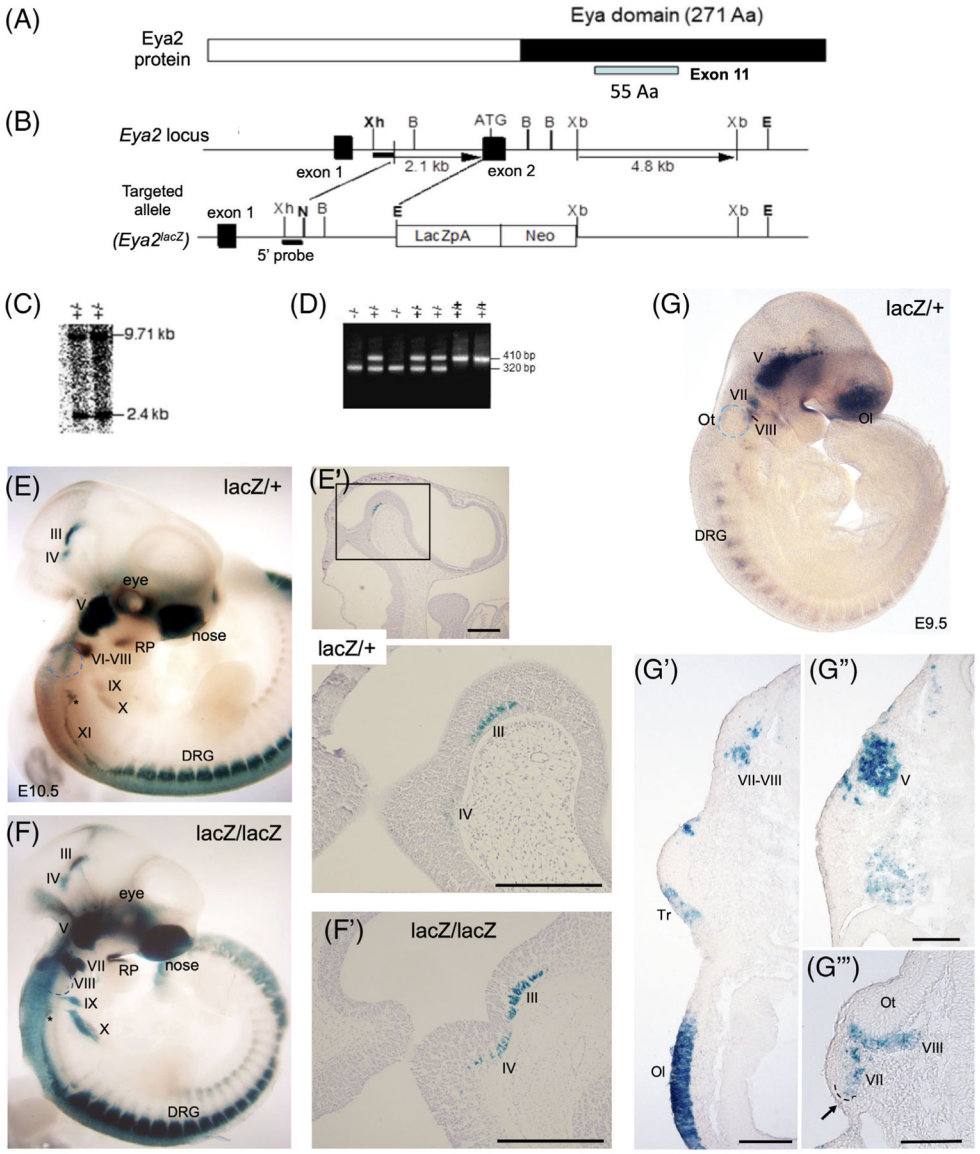

Figure 1.

Generation of *Eya2* knockout (KO) and *Eya2*^{lacZ} reporter knockin (KI) mice through gene targeting. A, Schematic diagram illustrating the Eya2 protein and targeted KO deletion of the 54 amino acids within the ED. B, Schematic diagram illustrating the *Eya2* locus and targeted *Eya2*^{lacZ} KI. The endogenous start codon and the exon 1 were replaced by *Escherichia coli* ATG-lacZ-poly(A) cassette and the *neo* positive selection cassette. C, Southern blot analysis of ES cell clones. Genomic DNA was digested with EcoRI and XhoI, and probes with the 5′ flanking probe (550-bp XhoI-NotI fragment) and the resulting wild-type band is 9.71-kb and the targeted band is 2.4-kb. D, Heterozygous or homozygous progeny were genotyped by PCR in a same reaction to amplify a 410-bp wild-type band and a 320-bp *lacZ* knockin band. E and F, β-Gal staining of *Eya2*^{lacZ} expression in heterozygous and homozygous mouse embryos at E10.5. E′ and F′, Sagittal sections showing β-Gal activity in the motor neurons of the oculomotor (III) and trochlear (IV)

nuclei. In panel E′, the bottom panel is the boxed area of the upper panel. G, Whole-mount β-Gal staining of *Eya2*^{lacZ} in heterozygous embryo at E9.5. Arrow points to cculomotor (III) and trochlear (IV) nerves. G′ and G″, Transverse sections of embryo shown in F. Arrow points to epibranchial placodal ectoderm (outlined by dashed line). V to X, cranial sensory ganglia Vth to Xth; DRG, dorsal root ganglion; Ot, otic vesicle; Ol, invaginating olfactory epithelium; RP, Ratheke's pouch; Tr, trigeminal placodal ectoderm. Scale bar: 250 μm (E′, F′) and 100 μm (G′, G″, G‴)

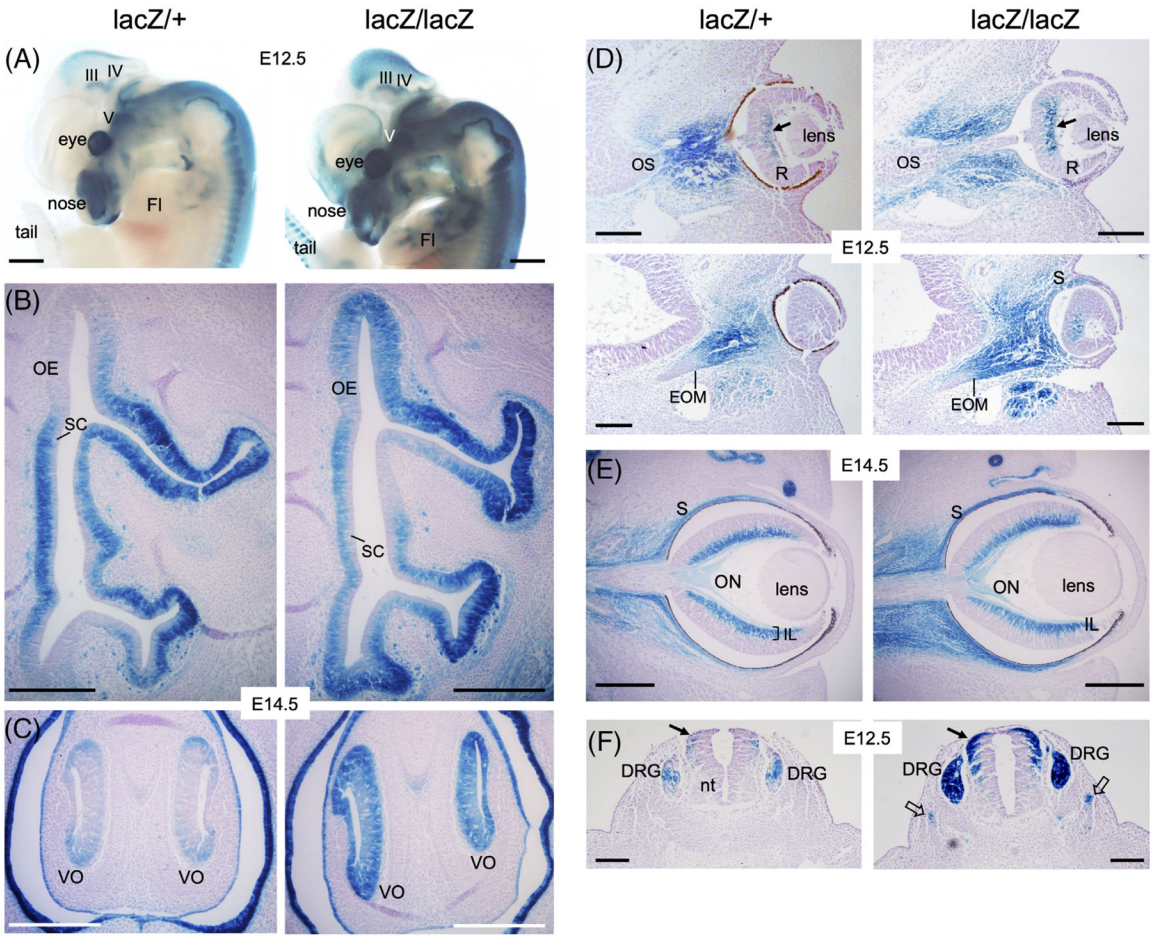

Figure 2.

Eya2^{lacZ} reporter is expressed in differentiating olfactory epithelium, retina, dorsal root ganglion and somite. A, Whole-mount X-gal staining of E12.5 embryos showing *Eya2*^{lacZ} expression in the cranial ganglia and nerves, olfactory system, eye and dorsal root ganglia and forelimb (Fl) in *Eya2*$^{lacZ/+}$ and *Eya2*$^{lacZ/lacZ}$. III/IV, oculomotor/trochlear nuclei; V, Vth ganglion. B and C, X-gal staining on transverse sections revealing *Eya2*^{lacZ} expression in the basal neuronal progenitors but not in the apical layer of sustentacular cells (SC) of the olfactory epithelium (OE) and vomeronasal organ (VNO) in *Eya2*$^{lacZ/+}$ and *Eya2*$^{lacZ/lacZ}$ at E14.5. D, X-gal staining at E12.5 showing β-Gal activity in mesenchymal cells surrounding optic stalk (OS), in extraocular muscles (EOM), in sclera (S) and inner layer (arrow) in the center of retina (R) in both heterozygotes and homozygotes. E, At E14.5, β-Gal activity was similarly detected in the sclera and inner layer (IL) of the retina and weakly in the optic nerve (ON) in both heterozygotes and homozygotes. F, X-gal staining showing β-Gal activity in dorsal root ganglion (DRG) and dorsal neural tube (arrows) in *Eya2*$^{lacZ/+}$ and with stronger intensity in *Eya2*$^{lacZ/lacZ}$, in which β-Gal activity also became detectable in somite (open arrows). Scale bar: 500 μm (A) and 150 μm (B–F)

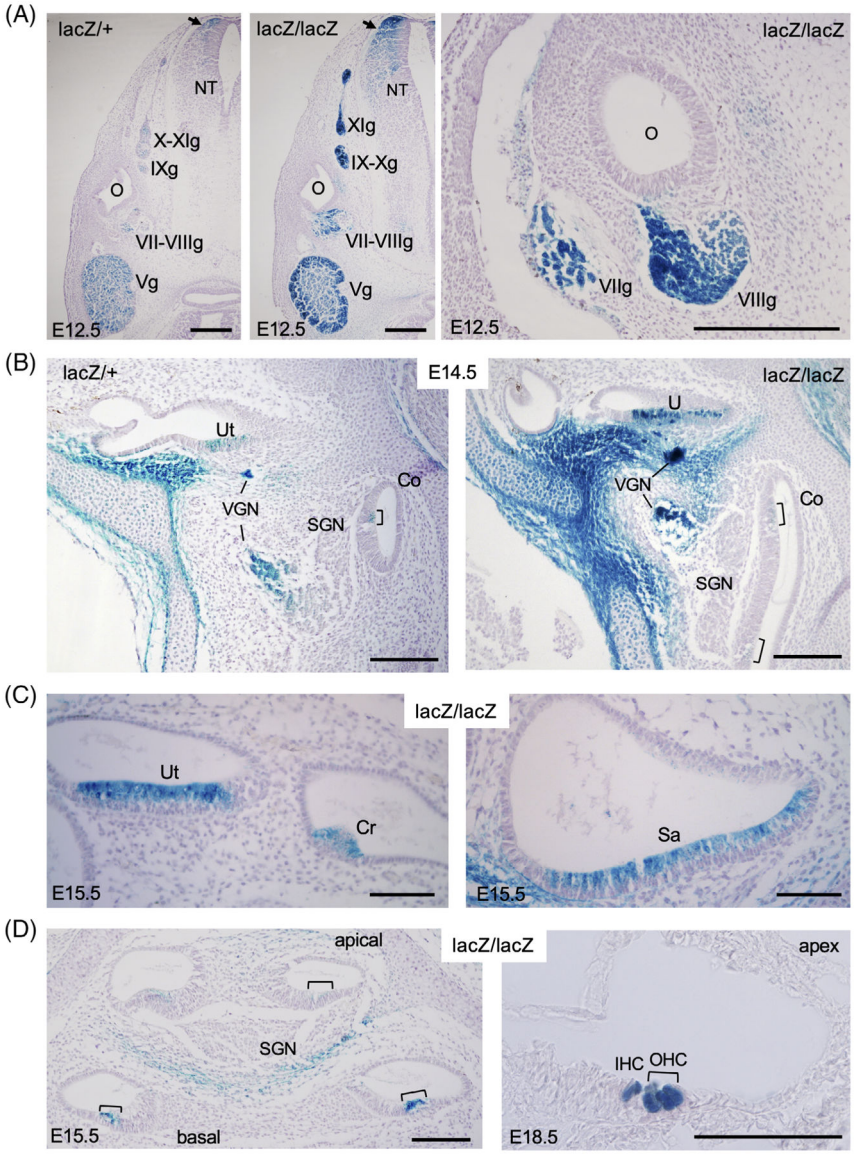

Figure 3.

Eya2^{lacZ} reporter is expressed in differentiating sensory hair cells in all six sensory epithelia of the inner ear. A, X-gal staining revealing β-Gal activity in Vth–XIth ganglia (Vg-XIg and dorsal neural tube (arrow) at E12.5. O, otic/inner ear; NT, neural tube. B, At E14.5, β-Gal activity was detected in vestibular ganglion neurons (VGN) and differentiating hair cells in utricle (U) and faintly in the hair cells of the organ of Corti (brackets) of the basal cochlea (Co) in both *Eya2*$^{lacZ/+}$ and *Eya2*$^{lacZ/lacZ}$. C, At E15.5, β-Gal activity was detected differentiating hair cells in all vestibular sensory epithelia, including utriclar macula (Ut), cristae ampullaris (Cr), sacullar macula (Sa). D, In the cochlea, stronger β-Gal activity was observed in the basal turn but weaker in the apical turns of the organ of Corit (brackets) at E15.5 and by E18.5, stronger β-Gal activity was observed in both inner (IHC) and outer hair cells (OHC) throughout the cochlear duct. Scale bar: 300 μm (A), 150 μm (B), 75 μm (C), and 100 μm (D)

(A) **Preyer reflex and behavioral test**

Phenotype	No. of animals tested (4 weeks old)	
	Eya2$^{lacZ/+}$ (13)	*Eya2*$^{lacZ/lacZ}$ (9)
Abnormal Preyer reflex response	0	4
Circling response	0	0
Headtossing	0	0
Abnormal swimming response	0	0

(B)

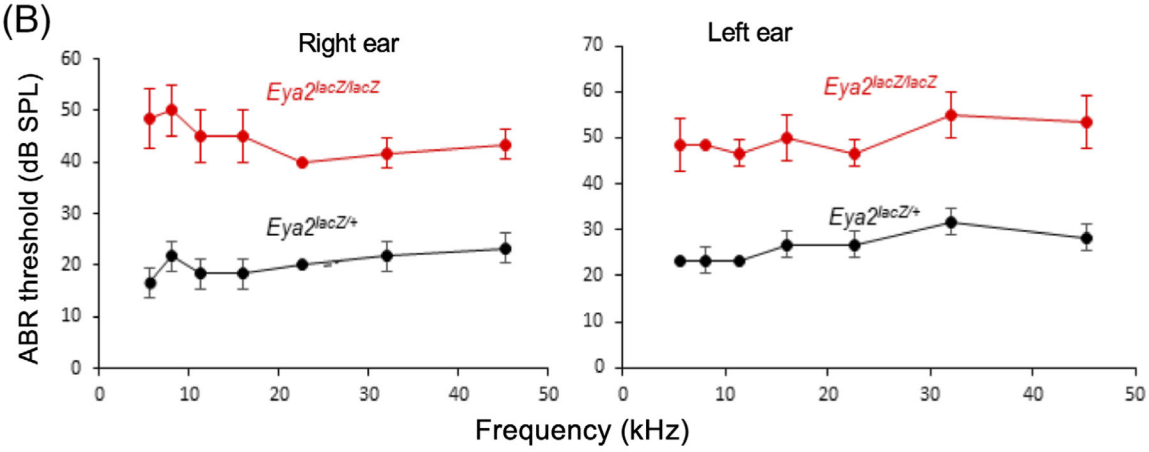

Figure 4.

Eya2$^{lacZ/lacZ}$ mice show mild hearing loss. A, Gross and behavioral abnormalities of *Eya2*$^{lacZ/+}$ and *Eya2*$^{lacZ/lacZ}$ mice. B, ABR threshold measurements of 8 weeks old mice. Three *Eya2*$^{lacZ/lacZ}$ mice (one male and two females) that had no ABR response were not included. Average threshold ± s.e.m. for *Eya2*$^{lacZ/+}$ (n = 5) and *Eya2*$^{lacZ/lacZ}$ (n = 7) ears at 8 weeks of age (threshold shift by 20 to 31 dB in right ear and 20 to 25 dB in left ear of homozygotes)

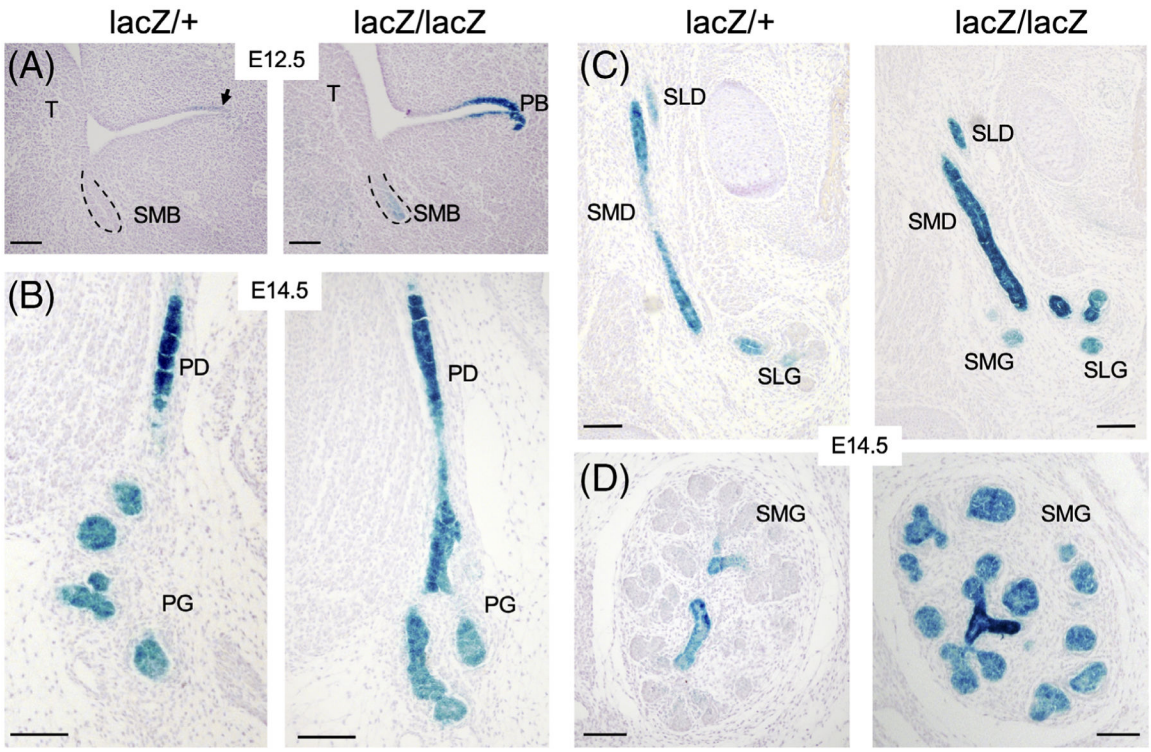

Figure 5.

Eya2^{lacZ} reporter gene expression in salivary gland. A, X-gal staining on sections at E12.5 showing β-Gal-activity weaker in submandibular bud (SMB) and stronger in parotid bud (PB) in *Eya2*$^{lacZ/lacZ}$ but only faint β-Gal-activity in parotid bud in *Eya2*$^{lacZ/+}$. B, At E14.5, stronger β-Gal activity in parotid duct (PD) and weaker in branching parotid gland (PD) in both *Eya2*$^{lacZ/+}$ and *Eya2*$^{lacZ/lacZ}$. C and D, Similarly, stronger β-Gal activity in submandibular (SMD) and sublingual duct (SLD) and relatively weaker in branching submandibular (SMG) and sublingual gland (SLG). Scale bar: 100 μm

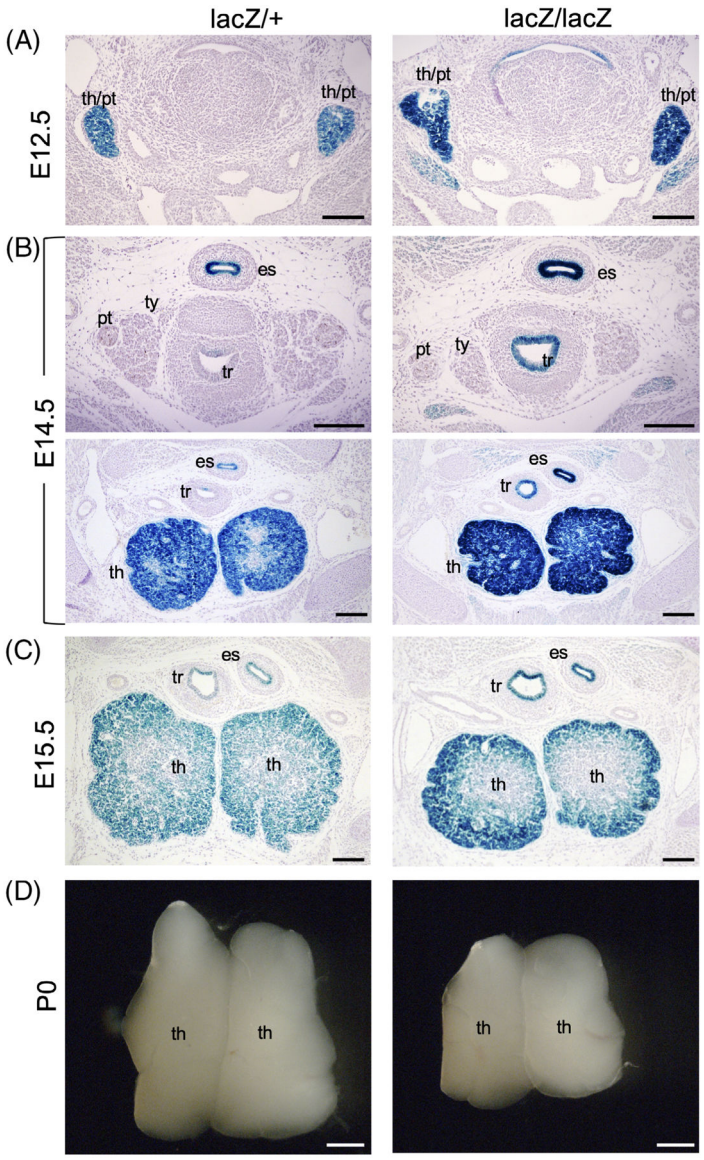

Figure 6.

Eya2^{lacZ} reporter gene expression in thymus and reduced size of thymus lobes associated with *Eya2*-deficincy. A and B, Transverse sections showing that in *Eya2*$^{lacZ/+}$ embryos, the third pouches evaginate and then separate as buds to form the primordia of thymus/parathyroid (th/pt) at around E12.5. *Eya2* was detected in the th/pt at E12.5 (A), E14.5 thymus lobes (th), trachea (tr) and esophagus (es) (B). C, At E15.5, *Eya2* expression was detected in the two thymus lobes, esophagus and trachea in *Eya2*$^{lacZ/+}$ and *Eya2*$^{lacZ/lacZ}$ embryos. D, Whole thymus lobes in *Eya2*$^{lacZ/+}$ embryos (G) and *Eya2*$^{lacZ/lacZ}$ embryos (H) at P0. Scale bar: 150 μm (A–C) and 500 μm (D)